

1 *Streptococcus agalactiae* induces placental macrophages to release extracellular traps loaded with
2 tissue remodeling enzymes via an oxidative-burst-dependent mechanism
3

4 Ryan S. Doster^a, Jessica A. Sutton^b, Lisa M. Rogers^a, David M. Aronoff^{ff^{a,b,c,d}}, and Jennifer A.
5 Gaddy^{a,e,#}
6

7 ^aDivision of Infectious Diseases, Department of Medicine, Vanderbilt University Medical Center,
8 Nashville, Tennessee, U.S.A.

9 ^bDepartment of Microbiology and Immunology, Meharry Medical College, Nashville, Tennessee,
10 U.S.A.

11 ^cDepartment of Obstetrics and Gynecology, Vanderbilt University Medical Center, Nashville,
12 Tennessee, U.S.A.

13 ^dDepartment of Pathology, Microbiology and Immunology, Vanderbilt University Medical Center,
14 Nashville, Tennessee, U.S.A.

15 ^eTennessee Valley Healthcare Systems, Department of Veterans Affairs, Nashville, Tennessee,
16 U.S.A.
17

18 Running Title: Placental macrophages release METs in response to GBS
19

20 Keywords: macrophage extracellular traps, GBS, matrix metalloproteinase
21

22 #Address correspondence to Jennifer A. Gaddy, Ph.D., jennifer.a.gaddy@vumc.org

23 J.A.G and D.M.A contributed equally to this work.
24

25 Abstract word count: 214

26 Text word count: 5858

27 **Abstract:**

28 *Streptococcus agalactiae*, or Group B *Streptococcus* (GBS), is a common perinatal pathogen. GBS
29 colonization of the vaginal mucosa during pregnancy is a risk factor for invasive infection of the fetal
30 membranes (chorioamnionitis) and its consequences such as membrane rupture, preterm labor,
31 stillbirth, and neonatal sepsis. Placental macrophages, or Hofbauer cells, are fetally-derived
32 macrophages present within placental and fetal membrane tissues that perform vital functions for fetal
33 and placental development, including supporting angiogenesis, tissue remodeling, and regulation of
34 maternal-fetal tolerance. Although placental macrophages, as tissue-resident innate phagocytes, are
35 likely to engage invasive bacteria such as GBS, there is limited information regarding how these cells
36 respond to bacterial infection. Here, we demonstrate *in vitro* that placental macrophages release
37 macrophage extracellular traps (METs) in response to bacterial infection. Placental macrophage
38 METs contain proteins including histones, myeloperoxidase, and neutrophil elastase similar to
39 neutrophil extracellular traps and are capable of killing GBS cells. MET release from these cells
40 occurs by a process that depends on the production of reactive oxygen species. Placental
41 macrophage METs also contain matrix metalloproteases that are released in response to GBS and
42 could contribute to fetal membrane weakening during infection. MET structures were identified within
43 human fetal membrane tissues infected *ex vivo*, suggesting that placental macrophages release
44 METs in response to bacterial infection during chorioamnionitis.

45

46 **Importance:**

47 *Streptococcus agalactiae*, also known as Group B *Streptococcus* (GBS), is a common pathogen
48 during pregnancy where infection can result in chorioamnionitis, preterm premature rupture of
49 membranes (PPROM), preterm labor, stillbirth, and neonatal sepsis. Mechanisms by which GBS
50 infection results in adverse pregnancy outcomes are still incompletely understood. This study
51 evaluated interactions between GBS and placental macrophages. The data demonstrate that in
52 response to infection, placental macrophages release extracellular traps capable of killing GBS.

53 Additionally, this work establishes that proteins associated with extracellular trap fibers include
54 several matrix metalloproteinases that have been associated with chorioamnionitis. In the context of
55 pregnancy, placental macrophage responses to bacterial infection might have beneficial and adverse
56 consequences, including protective effects against bacterial invasion but also releasing important
57 mediators of membrane breakdown that could contribute to membrane rupture or preterm labor.

58

59 **Introduction:**

60 15 million cases of preterm birth, or birth before 37 weeks gestation, occur annually worldwide,
61 including 500,000 cases in the United States, conferring an estimated cost of \$26.2 billion (1-3). The
62 World Health Organization estimates that preterm birth complications are a leading cause of death
63 among children under five years of age, resulting in nearly 1 million deaths in 2015 (4, 5). In addition
64 to loss of child lives, preterm birth increases risk of chronic health conditions including
65 neurodevelopmental deficits, metabolic syndrome, cardiovascular abnormalities, chronic kidney
66 disease, and chronic respiratory conditions (6, 7).

67 *Streptococcus agalactiae*, also known as Group B *Streptococcus* (GBS), is a common
68 perinatal pathogen (8). Approximately 10-40% of women are colonized with GBS during late
69 pregnancy (9, 10). Rectovaginal GBS carriage is associated with adverse pregnancy outcomes
70 including stillbirth, preterm labor, chorioamnionitis, and neonatal sepsis (11-13). Because of the
71 burden and severity of GBS-related adverse pregnancy outcomes, the CDC recommends GBS
72 screening late in gestation and antibiotic prophylaxis during labor (14). This strategy has decreased
73 the incidence of early-onset neonatal sepsis but misses mothers that deliver preterm, before
74 screening is conducted (14). Despite screening and treatment interventions, GBS remains a leading
75 neonatal pathogen (15).

76 Pregnancy represents a unique immunologic state in which the maternal immune system must
77 dampen its responses against foreign antigens of the semiallogenic fetus while defending the gravid
78 uterus from infection. Excessive inflammation can drive adverse pregnancy events including loss of

79 pregnancy, preterm birth, intrauterine growth restriction, and preeclampsia (16). Multiple mechanisms
80 exist to support maternal-fetal tolerance including production of anti-inflammatory cytokines that alter
81 the number and function of immune cells at the maternal-fetal interface (17-19). Unfortunately,
82 infection is a common complication of pregnancy. Bacterial infection of the fetal membranes, known
83 as chorioamnionitis, occurs most often by ascending infection from the vagina (8, 20, 21). During
84 infection, bacterial products are recognized by pathogen recognition receptors, which then stimulate
85 production of proinflammatory cytokines (20, 22, 23). These inflammatory mediators initiate a
86 cascade of events that result in neutrophil infiltration into the fetal membranes, production and
87 release of matrix metalloproteases (MMPs), and cervical contractions which eventually result in
88 membrane rupture and preterm birth (24).

89 Macrophages represent 20-30% of the leukocytes within gestational tissues (25). In particular,
90 fetally-derived macrophages, called Hofbauer cells or placental macrophages (PMs), play key roles in
91 placental invasion, angiogenesis, tissue remodeling, and development (26, 27). The inflammatory
92 state of these cells is carefully regulated throughout pregnancy. As the pregnancy progresses the M2
93 or anti-inflammatory and tissue remodeling phenotype predominates to supports fetal development
94 (28-31). PMs contribute to immune tolerance by secretion of anti-inflammatory cytokines, which
95 suppress production of proinflammatory cytokines (32-35). Disruption of appropriate macrophage
96 polarization is associated with abnormal pregnancies including spontaneous abortions, preterm labor,
97 and preeclampsia (28). We sought to understand how bacterial infection alters PM functions, and how
98 these responses may contribute to pathologic pregnancies. These studies demonstrate that both PMs
99 and a model macrophage cell line, the PMA-differentiated THP-1 macrophage-like cells, release
100 macrophage extracellular traps (METs) in response to bacterial infection in a process that is
101 dependent upon the generation of reactive oxygen species (ROS). METs, reminiscent of neutrophil
102 extracellular traps (NETs), have recently been recognized as structures released by macrophages
103 under a number of conditions including infection (36). PM METs contain histones, myeloperoxidase,

104 and neutrophils elastase as well as several MMPs, and MET structures are found within human fetal
105 membranes infected with GBS *ex vivo*.

107 **Results:**

108 **Placental macrophages release METs in response to GBS:**

109 To understand PM responses to GBS at the host-pathogen interface, isolated PMs were infected *ex*
110 *vivo* with GBS and cellular interactions examined using field-gun high-resolution scanning electron
111 microscopy (SEM). At one hour following infection, fine, reticular structures were noted extending
112 from macrophages, and these structures were less abundant in uninfected samples (Figure 1A, lower
113 panels). These structures resembled NETs. Recent reports suggest that macrophages also release
114 fibers composed of DNA and histones, known as METs (36, 37). To determine if these structures
115 were METs, macrophages were evaluated by scanning laser confocal microscopy after staining with
116 the DNA binding dye SYTOX Green, which demonstrated extracellular structures extending from PMs
117 that were not seen when PMs were treated with DNase I (Figure 1A, top panels). Cells were then
118 evaluated to assess the degree to which these structures contained proteins previously associated
119 with NETs and METs, including histones, myeloperoxidase, and neutrophil elastase (36, 37). Each of
120 these proteins co-localized to extracellular DNA structures extending from the PMs (Figure 1B). The
121 staining for MET-associated proteins was specific as no fluorescent signal was seen when either a
122 secondary conjugated antibody alone or an isotype control secondary conjugated antibody was used
123 to evaluate these structures (Sup. Figure 1). Together, these data suggest that these structures are
124 METs released by PMs. The extent of MET release was then quantified, and PMs co-cultured with
125 GBS released significantly more METs than uninfected cells and DNase I treatment degraded these
126 extracellular structures (Figure 1C). Additionally, MET release by PMs occurred in a dose dependent
127 fashion (Sup. Fig 2A), and MET release was not GBS strain or bacterial species specific as PMs
128 infected with GBS strain GB037, a capsular type V strain, *Escherichia coli*, or heat killed bacteria
129 resulted in similar MET release (Sup. Figure 3).

130 One major immunologic function of extracellular traps is the ability to immobilize and kill
131 microorganisms through the locally high concentration of cellular proteins including histones that have
132 antimicrobial effects (37, 38). In order to investigate the bactericidal activity of PM METs, PMs were
133 co-cultured with GBS cells alone or in the presence of DNase I. After 1 hour of infection, significantly
134 more bacterial colony forming units (CFU) were recovered from co-cultures treated with DNase I,
135 suggesting that PM METs have bactericidal activity and eliminating METs with DNase treatment
136 impaired bacterial killing (Figure 1D). To verify that DNase treatment itself did not result in significant
137 PM cell death, thus decreasing bactericidal ability, PMs were incubated with DNase I for one hour
138 prior to washing and stimulating PMs with heat-killed GBS for 24 hours. PM TNF- α release was used
139 as a marker of macrophage viability and function; there was no difference in TNF- α from supernatants
140 of cells treated with DNase compared to untreated cells (Sup. Figure 2B). Additionally, live-dead
141 bacterial staining of PMs infected with GBS demonstrated dead GBS cells adjacent to MET fibers
142 (Sup. Figure 2C). Together, these data provide evidence that PMs release METs in response to
143 bacteria and that these structures are capable of killing GBS cells.

144 Extracellular trap formation, or etosis, occurs by a cell death pathway distinct from pyroptosis
145 and apoptosis (39). To investigate if GBS infection results in different cell death pathways, GBS
146 infected PMs were assayed for LDH release as a marker of cellular death, TUNEL staining as a
147 marker of apoptosis, and IL-1 β release to indicate pyroptosis. At one hour of GBS infection,
148 supernatants of PMs co-cultured with GBS demonstrated an increase in macrophage death,
149 determined by LDH release (Sup. Figure 4A). However, GBS infected PMs did not exhibit a
150 significant difference in IL-1 β release or TUNEL positive cells compared to uninfected cells treated
151 with vehicle controls at 1 hour (Sup. Figure 4B-D).

152 **PMA-differentiated THP-1 macrophage-like cells release METs after direct bacterial contact:**

153 Experiments were conducted to determine if MET responses against GBS were specific to PMs or
154 might represent a broader macrophage response. The immortalized monocyte-like cell line, THP-1
155

156 cells, was evaluated after differentiation into macrophage-like cells with phorbol 12-myristate 13-
157 acetate (PMA) for 24 hours. THP-1 macrophage-like cells infected with GBS released significantly
158 more METs than uninfected cells, and DNase I treatment degraded the MET structures (Sup. Figure
159 5). The THP-1 MET response required contact with bacterial cells, as treatment of the macrophage-
160 like cells with sterile filtered bacterial culture supernatant did not stimulate MET release compared to
161 uninfected cells.

162 **Actin polymerization is required for GBS-induced MET release:**

163 Actin polymerization has been shown to be important for MET release (36). A similar role of
164 cytoskeletal changes on GBS-induced MET release in THP-1 macrophage-like cells was examined.
165 Treatment prior to infection with the actin polymerization inhibitor, cytochalasin D, but not nocodazole,
166 which inhibits microtubule polymerization, inhibited MET release compared to GBS infected,
167 untreated cells (Sup. Figure 5). As noted below (and shown in Figure 2B), cytochalasin D also
168 inhibited MET release by human PMs infected with GBS.

169 **Placental macrophage MET responses require ROS production:**

170
171 Neutrophil release of NETs occurs in a ROS-dependent manner (40). It was hypothesized that MET
172 release from PMs may require production of ROS. Treatment of PMs prior to infection with the
173 NADPH oxidase inhibitor diphenyleneiodonium (DPI) inhibited release of METs, whereas treatment of
174 uninfected macrophages with PMA resulted in similar levels of MET release to GBS infected cells
175 (Figure 2A, B). As with the THP-1 macrophage-like cells, treatment of PMs with cytochalasin D prior
176 to infection inhibited MET release. To further define that ROS production was associated with MET
177 release a fluorescent ROS dye was used to evaluate PMs for intracellular ROS production. Treatment
178 with DPI inhibited ROS production, and GBS infection as well as PMA treatment of uninfected PMs
179 resulted in significantly more ROS production than uninfected cells (Figure 2C, D). Interestingly,
180 pretreatment with cytochalasin D decreased levels of intracellular ROS production similar to that of
181

182 DPI, suggesting that pretreatment with the actin cytoskeletal inhibitor may actually be preventing MET
183 release by impeding ROS production. Additionally, ROS production in these experiments mirrored the
184 degree of MET release under similar conditions (Figure 2B), suggesting that ROS production is
185 necessary for MET release from these macrophages.

186
187 **Placental macrophage METs contain MMPs:** During pregnancy, PMs support gestational tissue
188 remodeling through release of MMPs. Because macrophage release of MMPs has been implicated in
189 the pathogenesis of fetal membrane rupture (41), we hypothesized that these proteases may also be
190 released in METs. Five MMPs that have been implicated in development and pathologic pregnancies
191 were evaluated. Immunofluorescent staining of METs was significant for the co-localization of MMP-1,
192 -7, -8, -9, and -12 with extracellular DNA structures (Figure 3A). As MMPs are present within METs
193 and GBS infection induced MET release, metalloprotease concentrations within co-culture
194 supernatants were examined to determine if GBS infection would result in an increase in
195 metalloprotease release. MMP-8 and MMP-9 have been investigated as potential biomarkers for
196 intrauterine infection (42-44), and concentrations of both were significantly elevated in supernatants
197 of GBS infected cells compared to uninfected controls (Figure 3B, C). Global MMP activity of co-
198 culture supernatants was then assessed to determine if the MMPs released were active by using a
199 MMP activity assay, which uses fluorescence resonance energy transfer peptides that, when cleaved
200 by MMPs, are fluorescent. Supernatants taken from placental macrophages co-cultured with GBS
201 demonstrated significantly more MMP activity compared to uninfected controls (Figure 3D). Together
202 these data suggest that PMs express several MMPs, and these MMPs are released during bacterial
203 infection within METs and into the extracellular spaces, where they might contribute to breakdown of
204 gestational tissue extracellular matrix.

205
206 **MET structures are present in human fetal membrane tissues infected *ex vivo*:** To determine if
207 METs were present within gestational tissues in response to infection, fetal membrane tissues from

208 healthy, term, non-laboring caesarian sections were obtained, excised, and organized into transwell
209 structures, creating two chambers separated by the fetal membranes. GBS cells were added to the
210 choriodecidual surface and infection was allowed to progress for 48 hours prior to fixing tissues for
211 immunohistochemistry and immunofluorescence analysis. CD163-positive cells were found localized
212 to an area of GBS microcolonies within the membranes that demonstrated histone staining extending
213 beyond the nucleus and into the extracellular space, suggesting the release of a MET-like structure
214 (Figure 4A). Immunofluorescence staining demonstrated CD163-positive cells associated with
215 extracellular material that stained positive for histones and MMP-9 (Figure 4B). Additional staining of
216 fetal membrane tissues using neutrophil elastase as was previously described for identification of
217 NETs in tissues (45), identified cells within the choriodecidia with long extensions that stained
218 strongly for neutrophil elastase that co-localized to histone H3 and DNA staining (Sup. Figure 6).
219 Cells releasing MET-like structures could be compared to cells with intact nuclei and neutrophil
220 elastase staining limited to granule structures suggesting that cells releasing MET-like structures had
221 undergone cellular changes consistent with etosis.

222

223 **Discussion:**

224 In the initial description of NETs in 2004, several potential immune functions were described including
225 the trapping and killing of microorganisms and degradation of bacterial products (37). Release of
226 cellular DNA and proteins within extracellular traps has also been associated with autoimmune
227 pathology in systemic lupus erythematosus and anti-neutrophil cytoplasmic autoantibodies (ANCA)-
228 associated vasculitis, as well as and in diseases of aseptic inflammation (46-50). Other leukocytes
229 including mast cells, eosinophils, basophils and macrophages have now been shown to release
230 extracellular trap structures (36, 51-54).

231 In this manuscript, PMs are added to a growing list of monocytes and tissue differentiated
232 macrophages capable of releasing METs, which includes human alveolar macrophages, glomerular
233 macrophages, peripheral blood monocytes, and macrophages from other mammalian and non-

234 mammalian species (36). These data demonstrate that human PMs and PMA-differentiated THP-1
235 macrophage-like cells release METs in response to bacterial infection and after treatment with the
236 protein kinase C agonist, PMA. The present data correlate with previous reports that neutrophils and
237 murine macrophages release traps in response to GBS infection and that METs are capable of killing
238 GBS cells (55, 56).

239 These data also demonstrate that PM METs contain many proteins previously identified in
240 NETs, including histones, neutrophil elastase, and myeloperoxidase (37). These results mirror other
241 MET investigations demonstrating that diverse macrophages produce and release proteins including
242 neutrophil elastase within MET structures. For example, human glomerular macrophages releasing
243 METs containing myeloperoxidase has been demonstrated in cases of ANCA-associated
244 glomerulonephritis and human alveolar macrophages have been shown to release METs containing
245 histones and MMP-9 (57, 58). Human blood monocytes release METs containing H3 histones,
246 myeloperoxidase, lactoferrin, and neutrophil elastase in response to *Candida albicans* cells, and
247 similar MET contents have been demonstrated in THP-1 macrophage-like cells infected with
248 *Mycobacterium massiliense* (59, 60).

249 Similar to neutrophil etosis, these data suggest that ROS generation is necessary for PM MET
250 release as this response was inhibited by treatment with the NADPH oxidase inhibitor, DPI. These
251 results mirror reports that inhibition of ROS production via chemical inhibitors resulted in diminished
252 MET release in bovine, caprine, murine, and human macrophages (61-65). In neutrophils, ROS act to
253 break down intracellular membranes and activates neutrophil elastase, which translocates to the
254 nucleus where it degrades histones and promotes chromatin decondensation (39). Myeloperoxidase
255 is thought to contribute chromatin decondensation by a enzymatic-independent mechanism (39). It is
256 unclear at this time if neutrophil elastase and myeloperoxidase perform similar roles in macrophages.

257 Our data indicate an increase in LDH release during infection, which is consistent with reports
258 that MET release results in cell death (66). Etosis has been noted to be distinct from other cellular
259 death pathways including pyroptosis and apoptosis. At one hour of infection when MET responses

were identified, there was no significant difference in TUNEL staining or IL-1 β release suggesting that PM METs occur by a distinct pathway. This is notable as previous reports have shown that the GBS toxin β -hemolysin is capable of inducing pyroptosis of macrophages, though in this study infection was allowed to progress for 4 hours, longer than that required for the PM MET response (67). Previous studies have also demonstrated that GBS is capable to inducing macrophage apoptosis, but again this occurred over longer periods of infection than the one hour that was capable of inducing MET responses (68).

Pretreatment of THP-1 macrophage-like cells and PMs with the actin cytoskeletal inhibitor, cytochalasin D, inhibited MET release, but not the microtubule inhibitor, nocodazole. Conflicting reports exist regarding the role of actin polymerization in etosis. Studies evaluating bovine macrophages and THP-1 cells demonstrated a decrease in MET release after cytochalasin treatment, but similar treatment of murine J744A.1 macrophage-like cells, RAW macrophage-like cells, and bovine blood monocytes did not have a significant effect on MET release (60, 61, 64, 69). This collection of conflicting reports mirrors the NET literature. In the original NET description, cytochalasin D prevented cell phagocytosis but not NET release (37). Others have documented NET inhibition with nocodazole or cytochalasin D in response to LPS or enrofloxacin (70, 71). Because of the differential responses, some authors have postulated that phagocytosis may be an important first step towards cell stimulation and ROS generation, and cytoskeletal inhibition may block the initial steps toward MET release. Another possibility is that the pretreatment with cytochalasin D may interrupt trafficking of the NADPH oxidase complex, thus impairing ROS production. NADPH oxidase is a complex of six components, and the cytosolic proteins p40^{phox} and p47^{phox} are known to interact with F-actin; treatment with cytochalasins have been shown to interrupt NADPH complex formation and lead to impaired ROS formation (72, 73). Timing of the cytochalasin treatment is important, as treatment of cells after pre-stimulation with molecules such as LPS, which stimulates NADPH oxidase assembly, may actually increase generation of ROS in these cells (74). In our study, macrophages were pretreated with cytochalasin D and were not stimulated prior to infection. It remains unclear if the

286 conflicting literature with regards to the impact of cytoskeletal inhibition on extracellular traps may be
287 explained by the timing of cytoskeletal inhibition and subsequent effects on ROS production.

288 PMs were found to produce and release several MMPs within MET structures. During
289 chorioamnionitis, inflammatory mediators lead to the production and release of several
290 metalloproteinases including MMP-1, MMP-7, MMP-8, and MMP-9 (75, 76). MMP-9 is considered to
291 be the major MMP responsible for collagenase activity within the membranes, but many other MMPs
292 are thought to contribute to the processes of membrane weakening (75, 77). This study reinforces
293 and expands previous reports that identified placental leukocytes as being able to secrete MMPs
294 including MMP-1, -7, and -9 (78). Several MMPs have been implicated in preterm birth and pathologic
295 pregnancies. MMP-1 and MMP-9 were found to be elevated in placental tissues of women with
296 preterm births compared to women delivering at full term (79). MMP-1 and neutrophil elastase have
297 been shown to stimulate uterine contractions (80). Interestingly, proteomic comparisons of amniotic
298 fluid from women with premature preterm rupture of membranes demonstrated increases in histones
299 (H3, H4, H2B), myeloperoxidase, neutrophil elastase, and MMP-9 in women with histologic
300 chorioamnionitis and proven intrauterine infection, which likely represents the influx of inflammatory
301 cells into these tissues and potentially release of extracellular traps (81). MMP-12, or macrophage
302 metalloelastase, is a key mediator of the breakdown of elastase and has been shown to be important
303 for spiral artery remodeling during parturition, but to date there are no studies demonstrating changes
304 in MMP-12 release during cases of pathologic pregnancies (82). MMP-12 is better studied in
305 conditions of lung pathology including emphysema, and alveolar macrophages are known to release
306 MMP-12 in METs during infection, suggesting that protease release from leukocytes may contribute
307 to this disease process (65). Analogous to a controlled burn, we speculate that tethering MMPs to
308 MET structures allows the host to control the release of these potent enzymes, thereby limiting their
309 capacity to broadly weaken membrane structure in response to infection.

310 MET release appears to occur within fetal membrane tissue as demonstrated by our
311 immunohistochemistry and immunofluorescence data. This report adds to the growing relevance of

312 these structures within cases of disease pathology. NETs have previously been identified in placenta
313 tissues from women with pregnancies complicated by systemic lupus erythematosus and
314 preeclampsia (83, 84). NETs were also found in fetal membrane samples of women with
315 spontaneous preterm labor due to acute chorioamnionitis (85). Interestingly, in this report, antibody
316 staining with histone H3 and neutrophil elastase was used to denote NET structures, but given our
317 data, this staining pattern would not have differentiated METs from NETs. Additionally, our group and
318 others have demonstrated that in animal models of vaginal colonization and perinatal infection with
319 GBS, neutrophils traffic to GBS-infected gestational tissues and release NETs containing
320 antimicrobial peptides including lactoferrin as a means to control bacterial growth and invasion (86-
321 88).

322 In conclusion, we demonstrate that placental macrophages as well as PMA-differentiated THP-
323 1 cells respond to bacterial infection by releasing METs. These MET structures contain proteins
324 similar to NETs, including histones, myeloperoxidase, and neutrophil elastase. MET release from
325 these macrophages can be stimulated in the absence of bacterial cells with PMA and is inhibited by
326 pathways that impair ROS production. Placental macrophage METs contain several MMPs that have
327 been implicated in pathologic pregnancies including premature rupture of membranes. MET
328 structures were identified in human fetal membrane tissue infected *ex vivo*. Together these results
329 suggest that placental macrophages, which are thought to help maintain maternal fetal tolerance and
330 aid in extracellular matrix remodeling, are capable of responding to GBS infection in a way that may
331 trap and kill GBS cells but may also release important mediators of fetal membrane extracellular
332 matrix digestion that could potentially contribute to infection related pathologies including preterm
333 rupture of membrane and preterm birth.

334 **Materials and Methods:**

335 **Placental macrophage isolation and culture:** Human placental macrophages (PM) and fetal
336 membrane tissues were isolated from placental tissues from women who delivered healthy infants at
337

338 full term by cesarean section (without labor). De-identified tissue samples were provided by the
339 Cooperative Human Tissue Network, which is funded by the National Cancer Institute. All tissues
340 were collected in accordance with Vanderbilt University Institutional Review Board (approval 131607).
341 Macrophage isolation occurred as previously described (89); briefly, placental villous tissue was
342 minced followed by digestion with DNase, collagenase, and hyaluronidase (all from Sigma-Aldrich, St.
343 Louis MO). Cells were filtered, centrifuged, and CD14⁺ cells were isolated using the magnetic MACS
344 Cell Separation system with CD14 microbeads (Miltenyi Biotec, Auburn CA). Cells were incubated in
345 in RPMI 1640 media (ThermoFisher, Waltham MA) with 10% charcoal stripped fetal bovine serum
346 (ThermoFisher) and 1% antibiotic/antimycotic solution (ThermoFisher) overnight at 37°C in 5%
347 carbon dioxide. The following day, PMs were suspended in RPMI media without antibiotic/antimycotic
348 and distributed into polystyrene plates. Cells were incubated for at least 1 hour prior to infection to
349 allow for cell adherence to plate or Poly-L-Lysine coated glass coverslips (Corning, Bedford MA) for
350 microscopy assays.

351
352 **THP-1 cell culture:** THP-1 cells (ATCC, Manassas VA) were cultured in RPMI 1640 media with 10%
353 charcoal treated FBS and 1% antibiotic/antimycotic media at 37°C in 5% carbon dioxide. 24-48 hours
354 prior to co-culture experiments, cells were treated with 100 nM phorbol 12-myristate 13-acetate
355 (PMA) (Sigma-Aldrich) to induce differentiation to macrophage-like cells. Prior to co-culture
356 experiments, cells were suspended in RPMI media without antibiotic/antimycotic and distributed into
357 polystyrene plates containing Poly-L-Lysine coated glass coverslips and allowed to rest for at least 1
358 hour prior to infection to promote cell adherence.

359
360 **Bacterial Culture:** *Streptococcus agalactiae* strain GB590 is a capsular type III, ST-17 strain isolated
361 from a woman with asymptomatic colonization (90), and GB037 is a capsular type V strain obtained
362 from a case of neonatal sepsis (91, 92). *Escherichia coli* serotype 075:H5:K1 is a clinical isolate
363 obtained from a fatal case of neonatal meningitis (93). Bacterial cells were cultured on tryptic soy

364 agar plates supplemented with 5% sheep blood (blood agar plates) at 37°C in ambient air overnight.
365 Bacteria were subcultured from blood agar plates into Todd-Hewitt broth or Luria Broth and incubated
366 under aerobic shaking conditions at 37°C in ambient air to stationary phase. Bacterial supernatant
367 was collected and sterile filtered using a 0.1 µm filter (Millipore Sigma, Burlington MA) and incubated
368 with THP-1 cells at a concentration of 10% volume. Bacterial cells were washed and suspended in
369 phosphate buffered saline (PBS, pH 7.4) and bacterial density was measured spectrophotometrically
370 at an optical density of 600 nm (OD₆₀₀) and bacterial numbers were determined with a coefficient of 1
371 OD₆₀₀ = 10⁹ CFU/mL.

372
373 **Bacterial-macrophage co-cultures:** PMs or PMA-differentiated macrophage-like cells in RPMI
374 without antibiotics were infected with GBS or *E. coli* cells at a multiplicity of infection (MOI) of 20:1
375 unless otherwise noted. Co-cultured cells were incubated at 37°C in air supplemented to 5% carbon
376 dioxide for 1 hour. As stated, some cells were pretreated with 10 µg/mL cytochalasin D
377 (ThermoFisher), 10 nM nocodazole, 100 Units/mL DNase I, 500 nM PMA, or 10µM
378 diphenyleneiodonium chloride (all from Sigma-Aldrich) for at least 20 minutes prior to infection. At 1
379 hour, supernatants were collected and cells were fixed with 2.0% paraformaldehyde and 2.5%
380 glutaraldehyde in 0.05 M sodium cacodylate buffer (Electron Microscopy Sciences, Hatfield PA) for at
381 least 12 hours prior to processing for microscopy.

382
383 **Field-emission gun scanning electron microscopy:** Following treatment and infection as above,
384 macrophages were incubated in 2.0% paraformaldehyde and 2.5% glutaraldehyde in 0.05 M sodium
385 cacodylate buffer for at least 12 hours prior to sequential dehydration with increasing concentrations
386 of ethanol. Samples were dried at the critical point, using a CO₂ drier (Tousimis, Rockville MD),
387 mounted onto an aluminum stub, and sputter coated with 80/20 gold-palladium. A thin strip of
388 colloidal silver was painted at the sample edge to dissipate sample charging. Samples were imaged
389 with an FEI Quanta 250 field-emission gun scanning electron microscope. Quantification of

390 macrophages producing extracellular traps was determined by evaluating scanning electron
391 micrograph images at 750X magnification and counting total macrophages and those macrophages
392 releasing extracellular traps. Extracellular traps were defined as previously described with typical
393 appearing fibers extending from the cell body into the extracellular space (36).

394
395 **Confocal Laser Scanning Microscopy:** Co-cultures were completed and macrophages fixed as
396 above. Coverslips were washed once with PBS prior to staining with SYTOX® Green (10 µM final
397 concentration, ThermoFisher) for double stranded DNA (dsDNA), and Hoechst 33342 (5 µM final
398 concentration, ThermoFisher) for condensed chromatin (nuclei). Additional staining for histones and
399 MMPs were accomplished by blocking cells in 1% bovine serum albumin in PBS for 30 minutes at
400 37°C followed by a 1 hour incubation at 37°C with antibodies for histone H3 (ab5103, abcam,
401 Cambridge, MA), neutrophil elastase (ab68672, abcam), myeloperoxidase (ab9535, abcam), matrix
402 metalloproteinase (MMP)-1 (ab551168, abcam), MMP-7 (ab5706, abcam), MMP-8 (ab81286,
403 abcam), MMP-9 (ab38898, abcam), or MMP-12 (ab137444, abcam). Cells were then washed 3 times
404 with 1% BSA in PBS followed by a 30 minute incubation with an Alexa-594 conjugated goat anti-
405 rabbit secondary antibody (ThermoFisher) and 2 additional washes with 1% BSA in PBS prior to
406 mounting coverslips onto glass microscope slides with Aqua Poly/Mount (Polysciences Inc,
407 Warrington PA). Macrophages were visualized with a Zeiss LSM 710 META Inverted Laser Scanning
408 Confocal Microscope, and extracellular traps were identified by dsDNA staining that extended into the
409 extracellular environment.

410
411 **Bacterial killing by macrophages releasing extracellular traps:** PMs were infected with GBS cells
412 at an MOI of 20:1 as described above. As indicated some PMs were incubated with 100 U/mL DNase
413 I during infection to degrade extracellular trap structures as has been described previously (37). At
414 the end of 1 hour, DNase I was added to previously untreated wells for 10 minutes to release trapped
415 bacterial cells. Supernatants were collected and PMs were permeabilized with 0.05% Tween-20 in

sterile ice-cold water to release intracellular bacteria. Samples were vortexed vigorously, serially diluted, and plated on blood agar plates to enumerate bacterial cells. Untreated PMs were compared to DNase I treated cells and data are expressed as the percent colony forming units (CFU) recovered compared to untreated cells. To further evaluate bacterial killing, PMs were seeded onto coverslips and infected as above. Following infection, cells were stained using the Live/Dead BacLight Bacterial Viability Kit (Invitrogen) prior to confocal laser scanning microscopy.

LDH cytotoxicity assay: Placental macrophages were incubated in RPMI media without antibiotics or serum and infected as above. Supernatants were collected and centrifuged to pellet cellular debris. Supernatants were analyzed using the Cytotoxicity Detection Kit (Sigma-Aldrich) per manufacturer instructions. Results are expressed as percent toxicity using media without cells as the low control and cells treated with 2% Triton X as a high control. Percent cytotoxicity was calculated using the following equation: $\text{cytotoxicity (\%)} = (\text{experimental value} - \text{low control}) / (\text{high control} - \text{low control}) \times 100$.

Apoptosis Assay: Placental macrophages were incubated in RPMI media without antibiotics and infected as above. Following infection supernatants were removed and cells were fixed with 2.0% paraformaldehyde and 2.5% glutaraldehyde in 0.05 M sodium cacodylate buffer for at least 15 minutes. Click-iT Plus TUNEL Assay with Alexa-Fluor 594 dye (ThermoFisher) was used to identify cells undergoing apoptosis and staining was conducted per manufacturer instructions with additional staining that included Hoechst 33342 to visualize nuclei prior to confocal laser scanning microscopy.

Macrophage viability assay: To determine if DNase I treatment resulted in alterations in PM viability or function, TNF- α release was used a functional measure. Cells were left untreated or treated with 100 U/mL DNase I for 60 minutes. All cells were then washed and fresh media added prior to stimulation with 150:1 heat-killed GBS cells (incubated at 42°C for 2 hours) for 24 hours.

441 Supernatants were collected and centrifuged to pellet cellular debris before TNF- α release was
442 determined using a DuoSet TNF- α ELISA (R&D Systems) per manufacturer instructions.

443
444 **Measurement of intracellular ROS production:** Measurements of intracellular ROS production was
445 made by staining cells with CellRox® Deep Red Reagent (ThermoFisher) which measures oxidative
446 stress by producing fluorescence upon oxidation by ROS. PMs were isolated and treated as
447 described above. At the time of infection, a cellular stain mixture containing CellROX Deep Red (5 μ M
448 final concentration), SYTOX GREEN, and Hoechst 33342 was added to co-cultures. After 1 hour of
449 infection, cells were washed 3 times with PBS before a 15-minute fixation with 3.7% formaldehyde to
450 preserve CellRox Reagent signal. Coverslips were then mounted onto glass slides and visualized
451 with a visualized with a Zeiss LSM 710 confocal microscope as above. Images obtained were
452 analyzed using Fiji Version 1.0 (94). In order to quantify ROS production, a cellular ROS production
453 index was calculated using the following equation: $((\text{total image intensity} - (\text{mean background}$
454 $\text{fluorescence} \times \text{image area}))/\text{total macrophages counted}) \times (\text{number of macrophages with ROS}$
455 $\text{production}/\text{total macrophages counted})$. Images capturing only ROS staining (without other
456 stains/channels) were measured to determine the total corrected fluorescence for the total image
457 area. Mean background fluorescence was determined by at least 3 different measurements in areas
458 of the image lacking cellular contents (95). Data are presented as the mean \pm SE ROS cellular
459 production index of 10 images per sample.

460
461 **Metalloproteinase ELISA:** Supernatants from macrophage-GBS co-cultures were collected and
462 centrifuged as above to remove cellular debris. Supernatants were then evaluated for the
463 concentration of human MMP-8 and MMP-9 using DuoSet ELISA kits (R&D Systems, Minneapolis,
464 MN) per the manufacturer's protocol and protein levels were calculated from a standard curve.

465
466 **Matrix metalloproteinase activity:** MMP activity of co-culture supernatants was measured using the

467 MMP Activity Assay Kit (abcam). Supernatants were incubated with assay buffer for 30 minutes and
468 fluorescence signal was measured with a fluorescence microplate reader at an Ex/Em = 490/525 nm.
469 Sample values were normalized to uninfected cells from the same placental sample to calculate a
470 percent change for each placental sample assayed.

471 **Human fetal membrane infections:** Fetal membrane tissue was obtained and cultured as previously
472 described (96). Briefly, fetal membranes were excised from placental tissues. Fetal membrane tissue
473 sections were suspended over a 12 mm Transwell Permeable Support without membrane (Corning)
474 and immobilized using a ¼ inch intraoral elastic band (Ormco, Orange CA) so that the choriodecidua
475 was oriented facing up. Both transwell chambers were incubated with Dulbecco's modified Eagle's
476 medium (DMEM), high-glucose, HEPES, no-phenol-red cell culture medium (Gibco, Carlsbad,
477 California) supplemented with 1% fetal bovine serum and PEN-STREP antibiotic/antimycotic mixture
478 (Gibco). Transwells were incubated overnight at 37°C in ambient air containing 5% CO₂ before media
479 was replaced with DMEM, high-glucose, HEPES, no-phenol-red cell culture medium (lacking the
480 PEN-STREP antibiotic/antimycotic mixture). Bacterial cells were added to the choriodecidual surface
481 of the gestational membranes at a multiplicity of infection of 1×10^6 cells per transwell. Co-cultures
482 were incubated at 37°C in ambient air containing 5% CO₂ for 48 hours at which time membrane
483 tissues were fixed in 10% neutral buffered formalin prior to paraffin embedding.

484 **Human fetal membrane immunohistochemistry staining:** Tissues were cut to 5 µm sections and
485 multiple sections were placed on each slide for analysis. For immunohistochemistry, slides were
486 deparaffinized and heat induced antigen retrieval was performed on the Bond Max automated IHC
487 stainer (Leica Biosystems, Buffalo Grove IL) using their Epitope Retrieval 2 solution for 5-20 minutes.
488 Slides were incubated with a rabbit polyclonal anti-GBS antibody (abcam, ab78846), rabbit polyclonal
489 anti-histone H3 antibody (abcam, ab8580), or a mouse monoclonal anti-CD163 antibody (MRQ-26,
490 Cell Marque, Rocklin CA) for 1 hour. The Bond Polymer Refine detection system (Leica Biosystems)

491 was used for visualization. Slides were the dehydrated, cleared and coverslipped before light
492 microscopy analysis was performed.

493 **Human fetal membrane immunofluorescence staining:** For immunofluorescence evaluation of
494 METs within fetal membrane tissue, tissues were fixed and sectioned as above. Sections were briefly
495 incubated with xylene to deparaffinize. Tissues were blocked for greater than 1 hour with 10% bovine
496 serum albumins (Sigma-Aldrich) before staining with 1/100 dilutions of mouse monoclonal anti-H3
497 antibodies conjugated with Alexa Fluor® 647 (ab205729, abcam), rabbit monoclonal anti-CD163
498 antibodies conjugated with Alexa Fluor® 488 (ab218293, abcam), and mouse monoclonal anti-MMP-
499 9 antibodies conjugated with Alexa Fluor® 405 (NBP-259699AF405, Novus biological, Littleton CO)
500 overnight at room temperature. Additional tissues staining were conducted as previously described
501 (45). Tissues were deparaffinized and then incubated in R universal Epitope Recovery Buffer
502 (Electron Microscopy Sciences, Hatfield PA) at 50°C for 90 minutes. Samples were then rinsed in
503 deionized water three times followed by washing with TRIS-buffered saline (TBS, pH 7.4). Samples
504 were permeablized for 5 minutes with 0.5% Triton X100 in TBS at room temperature followed by 3
505 washes with TBS. Samples were then blocked with TBS with 10% BSA for 30 minutes prior to
506 incubation with 1:50 dilutions of rabbit poly-colonal anti-neutrophil elastase antibodies (481001,
507 MilliporeSigma, Burlington MA) and mouse monoclonal anti-H3 antibodies conjugated with Alexa
508 Fluor® 647 in blocking buffer at room temperature overnight. The following day, samples were
509 washed in TBS followed by repeat blocking with blocking buffer for 30 minutes at room temperature
510 before incubation with 1/00 dilution of Alexa Fluor® 488 conjugated donkey anti-rabbit IgG
511 (Invitrogen) for 4 hours at room temperature. Samples were then washed and incubated with 5 µM
512 Hoechst 33342 for 30 minutes to stain nuclei. After final washes, slides were dried and coverslipped.
513 Tissues were visualized with a Zeiss LSM 710 META Inverted Laser Scanning Confocal Microscope.
514 Images shown are representative of 4 separate experiments using tissues from different placental
515 samples.

516 **Statistics:** Statistical analysis of MET quantifications was performed using one-way ANOVA with
517 either Tukey's or Dunnet's post-hoc correction for multiple comparisons and all reported *p* values are
518 adjusted to account for multiple comparisons. MMP activities assays and bacterial killing assay were
519 normalized to untreated or uninfected cells and analyzed with Student's *t*-test or one-way ANOVA. *p*
520 values ≤ 0.05 were considered significant. All data analyzed in this work were derived from at least
521 three biological replicates (representing different placental samples). Statistical analyses were
522 performed using GraphPad Prism 6 for MAC OS X Software (Version 6.0g, GraphPad Software Inc.,
523 La Jolla CA).

524
525 **Acknowledgments:** The authors thank Dr. Oscar Gomez-Duarte and Dr. Shannon Manning for
526 providing the clinical bacterial isolates used in this study. The funders of this study had no role in
527 study design, data collection and interpretation, or the decision to submit the work for publication. The
528 authors have no conflicts of interest to disclose. Core Services including use of the Cell Imaging
529 Shared Resource were performed through support from Vanderbilt Institute for Clinical and
530 Translational Research program supported by the National Center for Research Resources, Grant
531 UL1 RR024975-01, and the National Center for Advancing Translational Sciences, Grant 2 UL1
532 TR000445-06. De-identified, human fetal membrane tissue samples were provided by the
533 Cooperative Human Tissue Network at Vanderbilt University, which is funded by the National Cancer
534 Institute.

536 Figure 1: Placental macrophages infected *ex vivo* with GBS release extracellular traps capable of
537 killing GBS cells. 1A: Placental macrophages were infected for 1 hour with GBS cells at an MOI of
538 20:1. Scanning electron micrographs (bottom row) demonstrate extracellular structures released from
539 macrophages (white arrows), which are not seen after DNase I treatment. PMs were also stained with
540 Sytox Green, a double stranded DNA dye, and evaluated by scanning laser confocal microscopy,
541 which demonstrates extracellular structures composed of DNA (white arrows). Measurement bars
542 represent 100 μm . 1B: Placental macrophage extracellular traps were stained with Hoechst 33342
543 (blue), a condensed chromatin/nuclear stain, SYTOX Green (green), and specific antibodies for either
544 histone H3, myeloperoxidase or neutrophil elastase as listed (red). Histone, myeloperoxidase and
545 neutrophil elastase staining co-localizes to extracellular DNA staining suggesting that MET structures
546 contain these proteins. Measurement bars represent 100 μm . 1C: PMs releasing METs were
547 quantified by counting MET producing cells seen in SEM images and expressed as the number of
548 macrophages releasing METs per field. GBS infected PMs release significantly more METs than
549 uninfected cells, and DNase I treatment degraded these structures. Data represent samples from 6-8
550 different placental samples, one-way ANOVA, $F = 32.7$, $p < 0.0001$, with post hoc Tukey's multiple
551 comparison test. 1D: Placental macrophage METs kill GBS cells. PMs were infected for 1 hour at
552 MOI 20:1 in the presence of DNase I to degrade METs or without (Untreated). Untreated wells were
553 treated with DNase I for the last 10 minutes of infection to break up DNA complexes prior to serial
554 dilution and plating. DNase I treatment significantly impairs bactericidal activity. Data represent the
555 percent recovered colony forming units (CFU), normalized to untreated cells from 7 separate
556 experiments from different placenta samples, Student's t test, $t = 3.224$, $df = 6$, $p = 0.0180$. ****
557 represents $p \leq 0.0001$, * represents $p \leq 0.05$.

558
559 Figure 2: MET release from placental macrophages requires ROS generation. Placental
560 macrophages were incubated with DNase I, DPI to inhibit ROS generation, or cytochalasin D to
561 prevent actin polymerization and then infected with GBS at an MOI of 20:1 for 1 hour. Uninfected

562 cells were also stimulated with 500 nM PMA to stimulate protein kinase C activation. 2A: Cells were
563 then imaged to identify MET release by confocal microscopy after staining with SYTOX green (top
564 row) or via SEM (bottom row). Measurement bars represent 100 μ m. 2B: MET release was then
565 quantified as in Figure 1. Treatment with DPI and cytochalasin D significantly inhibited MET release,
566 whereas MET release from PMA stimulated uninfected cells was not different from GBS infected
567 cells. Data represent mean \pm SE percent of cells releasing METs per field of 3-9 separate
568 experiments, one-way ANOVA, $F = 21.1$, $p < 0.0001$ with Tukey's multiple comparison test. 2C, D:
569 PM cell infections were repeated with staining for intracellular ROS production using CellROX deep
570 red reagent. This reagent becomes fluorescent when oxidized by ROS. Cells were co-cultured with
571 GBS cells as above and stained with CellROX deep red, SYTOX green, and Hoechst (2D top row).
572 Measurement bars represent 100 μ m. ROS production was quantified by measuring the total red
573 fluorescence per image (2D, bottom row) and the cellular ROS production index was calculated (2C).
574 Data are shown from a representative experiment of 3 independent experiments and are expressed
575 as the mean cellular ROS production index \pm SE of 10 images from a single placental sample. GBS
576 infected and PMA stimulated uninfected cells generated significantly higher amounts of ROS than
577 uninfected cells or those treated with DPI or cytochalasin D (one-way ANOVA, $F = 16.5$, $p < 0.0001$
578 with post hoc Tukey's multiple comparison test). **** represents $p \leq 0.0001$, *** represents $p \leq 0.001$,
579 ** represents $p \leq 0.01$, * represents $p \leq 0.05$.

580
581 Figure 3: GBS infection results in release of matrix metalloproteinases (MMPs) from placental
582 macrophages. 3A: PM METs contain MMP-1,- 7, -8, -9, and -12. PMs were infected as above and
583 then fixed and stained with anti-MMP antibodies and an Alexa Fluor-conjugated secondary antibody
584 (red), Hoechst 33342, and SYTOX green. METs (white arrows) stained strongly for MMPs.
585 Measurement bars represent 100 μ m. 3B, C: Supernatant from PM-GBS co-cultures were collected
586 and evaluated for MMP-8 (3B) and MMP-9 (3C) concentrations by ELISA. GBS infection results in a
587 significant increase in MMP-8 (Student's t test, $t = 3.599$, $df = 7$, $p = 0.0087$) and MMP-9 (Student's t

588 test, $t = 3.160$, $df = 10$, $p = 0.0102$) release compared to uninfected cells. 3D: PMs release active
589 MMPs in response to GBS. Supernatant from PM-GBS co-culture was evaluated for MMP activity
590 using a MMP Activity Assay to assess global MMP activity within co-culture supernatants.
591 Supernatant from GBS infected cells had 53% more MMP activity compared to uninfected PMs
592 (Student's t test, $t = 2.439$, $df = 11$, $p = 0.0329$).

593
594 Figure 4: Identification of MET-like structures within human fetal membrane tissues infected with GBS
595 *ex vivo*. Fetal membrane tissues were excised from healthy, term placental tissues from women
596 undergoing routine cesarean section. Fetal membrane tissues were then infected with GBS on the
597 choriondecidual surface for 48 hours prior to fixation and immunohistochemistry (4A) or confocal
598 microscopy (4B). 4A: Fetal membrane tissues were stained with hematoxylin and eosin (far left) and
599 representative images are shown at 4X magnification. Area within the red box is shown in sections
600 stained with anti-GBS, anti-CD163, or anti-histone H3 antibodies and visualized by
601 immunohistochemistry. GBS cells are able to invade from the choriondecidual surface (CD) toward the
602 amnion epithelium (AE). Macrophages are shown in the area of GBS infection and macrophages with
603 extracellular histone staining (far right, 40X insert) are demonstrated in an area that is also staining
604 with the macrophage marker CD163 (red boxes). Measurement bars represent 100 μm . 4B: Fixed
605 and paraffin embedded fetal membranes were stained with conjugated primary antibodies against
606 CD163, histone H3, and MMP-9. CD163-positive cells within the membrane tissue are seen extruding
607 contents that stain positive for histones and MMP-9 consistent with METs (white arrows).
608 Measurement bar represents 20 μm .

609
610 Figure S1: Staining controls for MET content evaluation. Placental macrophages were treated as in
611 Figure 1B, but were either stained without a primary antibody (top row) or with an isotype control
612 fluorophore-conjugated secondary antibody. Negligible myeloperoxidase (MPO) staining was

513 identified in these samples compared to Figure 1B (middle row) confirming the specificity of the
514 staining protocol. Measurement bars represent 100 μm .

515
516 Figure S2: GBS infection of PMs results in release of METs capable of killing GBS. S2A: PMs release
517 METs in a dose dependent response. PMs were infected for one hour at increasing MOI as indicated
518 or treated with vehicle control (PBS) (one-way ANOVA, $F = 12.3$, $p = 0.0076$ with post hoc Tukey's
519 multiple comparison test). S2B: DNase I treatment does not alter PM viability. PMs were either
520 treated with DNase I or left untreated for one hour before cells were washed and stimulated with heat-
521 killed GBS cells (MOI 150:1) or left unstimulated for 24 hours. Supernatants were assessed for TNF- α
522 release by ELISA as a measure of viability. Treatment of PMs with DNase I did not have a significant
523 effect on TNF- α release (one-way ANOVA, $F = 7.75$, $p = 0.0016$ with post hoc Tukey's multiple
524 comparison test). S2C: PM METs are capable of killing GBS cells. PM co-cultures were stained with
525 live-dead bacterial staining including Syto9 and propidium iodide. Both dyes stain DNA but propidium
526 iodide (red) is excluded from live cells. Dead GBS cells (red) are shown in close proximity to MET
527 fibers (white arrows). Measurement bar represents 50 μm .

528
529 Figure S3: Placental macrophages release extracellular traps in response to different GBS strains as
530 well as *E. coli* cells. S3A: Placental macrophages were co-cultured with live GBS strain GB037, *E.*
531 *coli* cells, or heat killed GBS or *E. coli* cells at an MOI of 20:1 for 1 hour. Cells were pretreated with
532 DNase I as indicated. Cells were then fixed and subsequently stained with SYTOX Green and
533 evaluated for MET release by confocal microscopy. Measurement bars represent 100 μm . S3B:
534 Placental macrophages releasing METs were quantified by counting MET producing cells from SEM
535 images (not shown) and expressed as the number of macrophages releasing METs per field. At 1
536 hour of infection live GB037, heat killed GB590 (GBS), and live or dead *E. coli* stimulated MET
537 release as DNase I treatment significantly reduced the number of extracellular structures (unpaired t -

538 test of similar treated groups of at least 3 separate experiments from separate placental samples). ***
539 represents $p \leq 0.001$, ** represents $p \leq 0.01$, * represents $p \leq 0.05$.
540
541 Figure S4: GBS infection results in PM cell death but not pyroptosis or apoptosis at 1 hour of
542 infection. PMs were isolated and co-cultured with GBS as in Figure 1. S4A: Following 1 hour of
543 infection, co-culture supernatants were assayed for LDH release and percent cytotoxicity was
544 calculated. GBS infection results in a significant increase in cell death (two-tailed, paired Student's t
545 test, $t = 4.13$, $df = 4$, $p = 0.0145$). S4B: GBS infection does not result in significant PM pyroptosis at 1
546 hour. Following infection as above, co-culture supernatants were assessed for IL-1 β release by
547 ELISA. GBS infection does not result in significant IL-1 β release (two-tailed Student's t test, $t =$
548 0.08945 , $df = 11$, $p = 0.9303$). S4C,D: Following infection as above, PMs underwent TUNEL staining
549 to evaluate cells for apoptotic changes. S4C: Representative confocal images demonstrate nuclear
550 staining (blue) and TUNEL positive cells (red, bottom row). Permeabilized, DNase I treated cells are
551 shown as a positive control. S4D: Quantification of TUNEL positive cells. One hour of GBS infection
552 does not result in an increase in TUNEL positive PMs (two-tailed, paired Student's t test, $t = 1.056$, df
553 $= 2$, $p = 0.4017$).
554
555 Figure S5: PMA activated THP-1 macrophage-like cells release METs in response to GBS. S5A:
556 THP-1 cells were incubated with 100 nM PMA for 24 hours prior to infection to induce differentiation
557 to macrophage-like cells. Cells were infected with GBS at an MOI of 20:1 for 1 hour. As indicated,
558 cells were pre-incubated with DNase I, cytochalasin D, nocodazole, or exposed to 10% volume of
559 sterile filtered bacterial supernatant from GBS cultures grown overnight to steady state. After
560 infection, cells were fixed and evaluated by confocal microscopy after staining with SYTOX Green
561 (top) or by SEM (bottom). White arrows denote METs. Measurement bars represent 100 μm . S5B:
562 Macrophages releasing METs were quantified by counting MET producing cells seen in SEM images
563 and expressed as the number of macrophages releasing METs per field. Data represent mean

percent of cells releasing METs per field of 3 separate experiments, one-way ANOVA, $F = 8.08$, $p = 0.028$ with Dunnett's multiple comparison test with samples compared to GBS infected. * represents $p < 0.05$, ** represents $p < 0.01$.

Figure S6: MET-like structures containing neutrophil elastase are seen in human fetal membrane tissues infected *ex vivo* with GBS. Human fetal membrane tissues were isolated and infected as in Figure 4 and then stained for neutrophil elastase (green), histones (red), or DNA/chromatin (blue). Neutrophil elastase positive cells were identified in the choriodecidua (CD) (top panel). The area in the red box was then evaluated at higher magnification and elongated structures of neutrophil elastase that co-localized with staining for histones and DNA consistent with METs were identified (white arrows). This staining pattern contrasts with staining of intact cells where neutrophil elastase staining was isolated to granule structures that did not localize to histone or DNA staining (yellow arrow). Measurement bars represent 20 μm .

579 Bibliography

- 580 1. Blencowe H, Cousens S, Chou D, Oestergaard M, Say L, Moller AB, Kinney M, Lawn J, Born
581 Too Soon Preterm Birth Action G. 2013. Born too soon: the global epidemiology of 15 million
582 preterm births. *Reprod Health* 10 Suppl 1:S2.
- 583 2. March of Dimes. 10/2013 2013. Permaternity Campaign, *on* March of Dimes.
584 <http://www.marchofdimes.org/mission/the-economic-and-societal-costs.aspx>. Accessed
585 1/21/2015.
- 586 3. WHO. 2012. Born Too Soon: The Global Action Report in Preterm Birth.
- 587 4. Organization WH. November 2016 2016. Preterm Birth: Fact Sheet, *on* WHO 2017.
588 <http://www.who.int/mediacentre/factsheets/fs363/en/>. Accessed 9/26/2017.
- 589 5. Liu L, Oza S, Hogan D, Chu Y, Perin J, Zhu J, Lawn JE, Cousens S, Mathers C, Black RE.
590 2016. Global, regional, and national causes of under-5 mortality in 2000-15: an updated
591 systematic analysis with implications for the Sustainable Development Goals. *Lancet*
592 388:3027-3035.
- 593 6. Luu TM, Rehman Mian MO, Nuyt AM. 2017. Long-Term Impact of Preterm Birth:
594 Neurodevelopmental and Physical Health Outcomes. *Clin Perinatol* 44:305-314.
- 595 7. Doyle LW. 2008. Cardiopulmonary outcomes of extreme prematurity. *Semin Perinatol* 32:28-
596 34.
- 597 8. Mendz GL, Kaakoush NO, Quinlivan JA. 2013. Bacterial aetiological agents of intra-amniotic
598 infections and preterm birth in pregnant women. *Front Cell Infect Microbiol* 3:58.
- 599 9. Kwatra G, Adrian PV, Shiri T, Buchmann EJ, Cutland CL, Madhi SA. 2014. Serotype-specific
700 acquisition and loss of group B streptococcus recto-vaginal colonization in late pregnancy.
701 *PLoS One* 9:e98778.
- 702 10. Russell NJ, Seale AC, O'Driscoll M, O'Sullivan C, Bianchi-Jassir F, Gonzalez-Guarin J, Lawn
703 JE, Baker CJ, Bartlett L, Cutland C, Gravett MG, Heath PT, Le Doare K, Madhi SA, Rubens
704 CE, Schrag S, Sobanjo-Ter Meulen A, Vekemans J, Saha SK, Ip M, Group GBSMCI. 2017.

- 705 Maternal Colonization With Group B Streptococcus and Serotype Distribution Worldwide:
706 Systematic Review and Meta-analyses. Clin Infect Dis 65:S100-S111.
- 707 11. Benitz WE, Gould JB, Druzin ML. 1999. Risk factors for early-onset group B streptococcal
708 sepsis: estimation of odds ratios by critical literature review. Pediatrics 103:e77.
- 709 12. Seale AC, Blencowe H, Bianchi-Jassir F, Embleton N, Bassat Q, Ordi J, Menendez C, Cutland
710 C, Briner C, Berkley JA, Lawn JE, Baker CJ, Bartlett L, Gravett MG, Heath PT, Ip M, Le Doare
711 K, Rubens CE, Saha SK, Schrag S, Meulen AS, Vekemans J, Madhi SA. 2017. Stillbirth With
712 Group B Streptococcus Disease Worldwide: Systematic Review and Meta-analyses. Clin Infect
713 Dis 65:S125-S132.
- 714 13. Bianchi-Jassir F, Seale AC, Kohli-Lynch M, Lawn JE, Baker CJ, Bartlett L, Cutland C, Gravett
715 MG, Heath PT, Ip M, Le Doare K, Madhi SA, Saha SK, Schrag S, Sobanjo-Ter Meulen A,
716 Vekemans J, Rubens CE. 2017. Preterm Birth Associated With Group B Streptococcus
717 Maternal Colonization Worldwide: Systematic Review and Meta-analyses. Clin Infect Dis
718 65:S133-S142.
- 719 14. Verani JR, McGee L, Schrag SJ, Division of Bacterial Diseases NCfl, Respiratory Diseases
720 CfDC, Prevention. 2010. Prevention of perinatal group B streptococcal disease--revised
721 guidelines from CDC, 2010. MMWR Recomm Rep 59:1-36.
- 722 15. BJ S, NI H, PJ S, RG F, BB P, KP VM, MJ B, RN G, ID F, EC H, S S, K K, WA C, KL W, EF B,
723 MC W, K S, AR L, AL S, SJ S, A D, RD H. 2011. Early Onset Neonatal Sepsis: The Burden of
724 Group B Streptococcal and E. coli Disease Continues. Pediatrics 127:817-826.
- 725 16. Ghaebi M, Nouri M, Ghasemzadeh A, Farzadi L, Jadidi-Niaragh F, Ahmadi M, Yousefi M.
726 2017. Immune regulatory network in successful pregnancy and reproductive failures. Biomed
727 Pharmacother 88:61-73.
- 728 17. Arck PC, Hecher K. 2013. Fetomaternal immune cross-talk and its consequences for maternal
729 and offspring's health. Nat Med 19:548-56.

- 730 18. Xu YY, Wang SC, Li DJ, Du MR. 2017. Co-Signaling Molecules in Maternal-Fetal Immunity.
731 Trends Mol Med 23:46-58.
- 732 19. Nagamatsu T, Barrier BF, Schust DJ. 2011. The regulation of T-cell cytokine production by
733 ICOS-B7H2 interactions at the human fetomaternal interface. Immunol Cell Biol 89:417-25.
- 734 20. Goldenberg RL, Hauth JC, Andrews WW. 2000. Intrauterine infection and preterm delivery. N
735 Engl J Med 342:1500-7.
- 736 21. Kim CJ, Romero R, Chaemsaihong P, Chaiyasit N, Yoon BH, Kim YM. 2015. Acute
737 chorioamnionitis and funisitis: definition, pathologic features, and clinical significance. Am J
738 Obstet Gynecol 213:S29-52.
- 739 22. Anders AP, Gaddy JA, Doster RS, Aronoff DM. 2017. Current concepts in maternal-fetal
740 immunology: Recognition and response to microbial pathogens by decidual stromal cells. Am J
741 Reprod Immunol doi:10.1111/aji.12623.
- 742 23. Stallmach T, Hebisch G, Joller H, Kolditz P, Engelmann M. 1995. Expression pattern of
743 cytokines in the different compartments of the feto-maternal unit under various conditions.
744 Reprod Fertil Dev 7:1573-80.
- 745 24. Agrawal V, Hirsch E. 2012. Intrauterine infection and preterm labor. Semin Fetal Neonatal Med
746 17:12-9.
- 747 25. Houser BL. 2012. Decidual macrophages and their roles at the maternal-fetal interface. Yale J
748 Biol Med 85:105-18.
- 749 26. Reyes L, Wolfe B, Golos T. 2017. Hofbauer Cells: Placental Macrophages of Fetal Origin.
750 Results Probl Cell Differ 62:45-60.
- 751 27. Brown MB, von Chamier M, Allam AB, Reyes L. 2014. M1/M2 macrophage polarity in normal
752 and complicated pregnancy. Front Immunol 5:606.
- 753 28. Zhang YH, He M, Wang Y, Liao AH. 2017. Modulators of the Balance between M1 and M2
754 Macrophages during Pregnancy. Front Immunol 8:120.

- 755 29. Mantovani A, Biswas SK, Galdiero MR, Sica A, Locati M. 2013. Macrophage plasticity and
756 polarization in tissue repair and remodelling. *J Pathol* 229:176-85.
- 757 30. Kim SY, Romero R, Tarca AL, Bhatti G, Kim CJ, Lee J, Elsey A, Than NG, Chaiworapongsa T,
758 Hassan SS, Kang GH, Kim JS. 2012. Methylome of fetal and maternal monocytes and
759 macrophages at the feto-maternal interface. *Am J Reprod Immunol* 68:8-27.
- 760 31. Gustafsson C, Mjosberg J, Matussek A, Geffers R, Matthiesen L, Berg G, Sharma S, Buer J,
761 Ernerudh J. 2008. Gene expression profiling of human decidual macrophages: evidence for
762 immunosuppressive phenotype. *PLoS One* 3:e2078.
- 763 32. Johnson EL, Chakraborty R. 2012. Placental Hofbauer cells limit HIV-1 replication and
764 potentially offset mother to child transmission (MTCT) by induction of immunoregulatory
765 cytokines. *Retrovirology* 9:101.
- 766 33. Chen CP, Tsai PS, Huang CJ. 2012. Antiinflammation effect of human placental multipotent
767 mesenchymal stromal cells is mediated by prostaglandin E2 via a myeloid differentiation
768 primary response gene 88-dependent pathway. *Anesthesiology* 117:568-79.
- 769 34. Montero J, Gomez-Abellan V, Arizcun M, Mulero V, Sepulcre MP. 2016. Prostaglandin E2
770 promotes M2 polarization of macrophages via a cAMP/CREB signaling pathway and
771 deactivates granulocytes in teleost fish. *Fish Shellfish Immunol* 55:632-41.
- 772 35. Wetzka B, Clark DE, Charnock-Jones DS, Zahradnik HP, Smith SK. 1997. Isolation of
773 macrophages (Hofbauer cells) from human term placenta and their prostaglandin E2 and
774 thromboxane production. *Hum Reprod* 12:847-52.
- 775 36. Doster RS, Rogers LM, Gaddy JA, Aronoff DM. 2018. Macrophage Extracellular Traps: A
776 Scoping Review. *J Innate Immun* 10:3-13.
- 777 37. Brinkmann V, Reichard U, Goosmann C, Fauler B, Uhlemann Y, Weiss DS, Weinrauch Y,
778 Zychlinsky A. 2004. Neutrophil extracellular traps kill bacteria. *Science* 303:1532-5.
- 779 38. Hirsch JG. 1958. Bactericidal action of histone. *J Exp Med* 108:925-44.

- 780 39. Papayannopoulos V, Metzler KD, Hakkim A, Zychlinsky A. 2010. Neutrophil elastase and
781 myeloperoxidase regulate the formation of neutrophil extracellular traps. *J Cell Biol* 191:677-
782 91.
- 783 40. Stoiber W, Obermayer A, Steinbacher P, Krautgartner WD. 2015. The Role of Reactive
784 Oxygen Species (ROS) in the Formation of Extracellular Traps (ETs) in Humans. *Biomolecules*
785 5:702-23.
- 786 41. Gomez-Lopez N, StLouis D, Lehr MA, Sanchez-Rodriguez EN, Arenas-Hernandez M. 2014.
787 Immune cells in term and preterm labor. *Cell Mol Immunol* 11:571-81.
- 788 42. Chaemsaitong P, Romero R, Docheva N, Chaiyasit N, Bhatti G, Pacora P, Hassan SS, Yeo
789 L, Erez O. 2018. Comparison of rapid MMP-8 and interleukin-6 point-of-care tests to identify
790 intra-amniotic inflammation/infection and impending preterm delivery in patients with preterm
791 labor and intact membranes(). *J Matern Fetal Neonatal Med* 31:228-244.
- 792 43. Kim KW, Romero R, Park HS, Park CW, Shim SS, Jun JK, Yoon BH. 2007. A rapid matrix
793 metalloproteinase-8 bedside test for the detection of intraamniotic inflammation in women with
794 preterm premature rupture of membranes. *Am J Obstet Gynecol* 197:292 e1-5.
- 795 44. Angus SR, Segel SY, Hsu CD, Locksmith GJ, Clark P, Sammel MD, Macones GA, Strauss JF,
796 3rd, Parry S. 2001. Amniotic fluid matrix metalloproteinase-8 indicates intra-amniotic infection.
797 *Am J Obstet Gynecol* 185:1232-8.
- 798 45. Brinkmann V, Abu Abed U, Goosmann C, Zychlinsky A. 2016. Immunodetection of NETs in
799 Paraffin-Embedded Tissue. *Front Immunol* 7:513.
- 800 46. Simon D, Simon HU, Yousefi S. 2013. Extracellular DNA traps in allergic, infectious, and
801 autoimmune diseases. *Allergy* 68:409-16.
- 802 47. Soderberg D, Segelmark M. 2016. Neutrophil Extracellular Traps in ANCA-Associated
803 Vasculitis. *Front Immunol* 7:256.

- 304 48. Delgado-Rizo V, Martinez-Guzman MA, Iniguez-Gutierrez L, Garcia-Orozco A, Alvarado-
305 Navarro A, Fafutis-Morris M. 2017. Neutrophil Extracellular Traps and Its Implications in
306 Inflammation: An Overview. *Front Immunol* 8:81.
- 307 49. Fuchs TA, Brill A, Duerschmied D, Schatzberg D, Monestier M, Myers DD, Jr., Wroblewski SK,
308 Wakefield TW, Hartwig JH, Wagner DD. 2010. Extracellular DNA traps promote thrombosis.
309 *Proc Natl Acad Sci U S A* 107:15880-5.
- 310 50. Schorn C, Janko C, Krenn V, Zhao Y, Munoz LE, Schett G, Herrmann M. 2012. Bonding the
311 foe - NETting neutrophils immobilize the pro-inflammatory monosodium urate crystals. *Front*
312 *Immunol* 3:376.
- 313 51. Mollerherm H, von Kockritz-Blickwede M, Branitzki-Heinemann K. 2016. Antimicrobial Activity
314 of Mast Cells: Role and Relevance of Extracellular DNA Traps. *Front Immunol* 7:265.
- 315 52. Yousefi S, Gold JA, Andina N, Lee JJ, Kelly AM, Kozlowski E, Schmid I, Straumann A,
316 Reichenbach J, Gleich GJ, Simon HU. 2008. Catapult-like release of mitochondrial DNA by
317 eosinophils contributes to antibacterial defense. *Nat Med* 14:949-53.
- 318 53. Morshed M, Hlushchuk R, Simon D, Walls AF, Obata-Ninomiya K, Karasuyama H, Djonov V,
319 Eggel A, Kaufmann T, Simon HU, Yousefi S. 2014. NADPH oxidase-independent formation of
320 extracellular DNA traps by basophils. *J Immunol* 192:5314-23.
- 321 54. von Kockritz-Blickwede M, Goldmann O, Thulin P, Heinemann K, Norrby-Teglund A, Rohde M,
322 Medina E. 2008. Phagocytosis-independent antimicrobial activity of mast cells by means of
323 extracellular trap formation. *Blood* 111:3070-80.
- 324 55. Vega VL, Crotty Alexander LE, Charles W, Hwang JH, Nizet V, De Maio A. 2014. Activation of
325 the stress response in macrophages alters the M1/M2 balance by enhancing bacterial killing
326 and IL-10 expression. *J Mol Med (Berl)* 92:1305-17.
- 327 56. Carlin AF, Uchiyama S, Chang YC, Lewis AL, Nizet V, Varki A. 2009. Molecular mimicry of
328 host sialylated glycans allows a bacterial pathogen to engage neutrophil Siglec-9 and dampen
329 the innate immune response. *Blood* 113:3333-6.

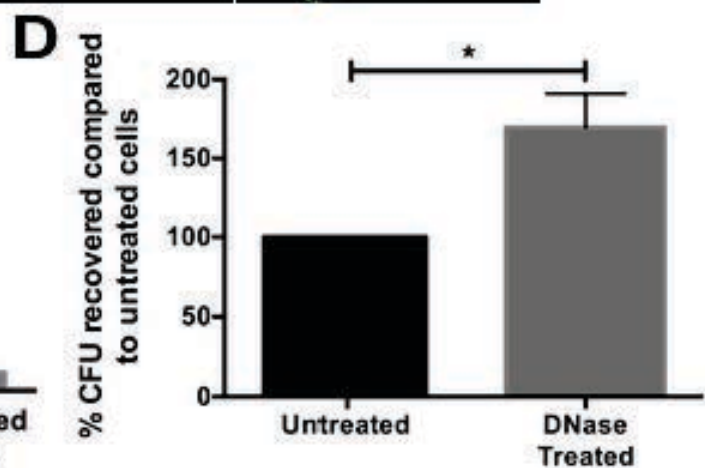
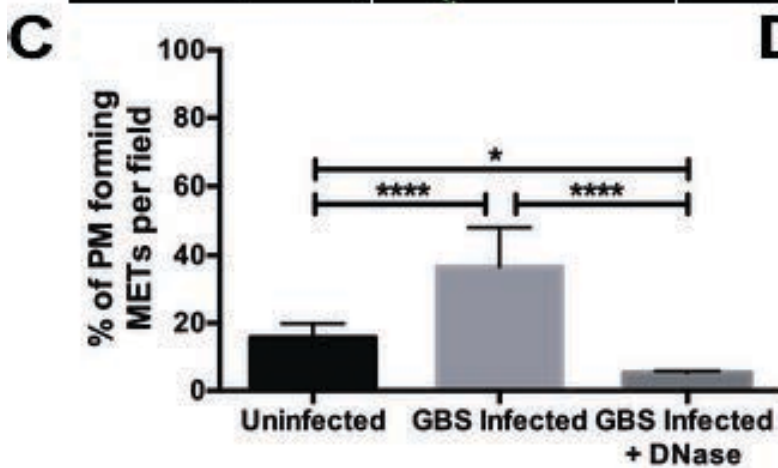
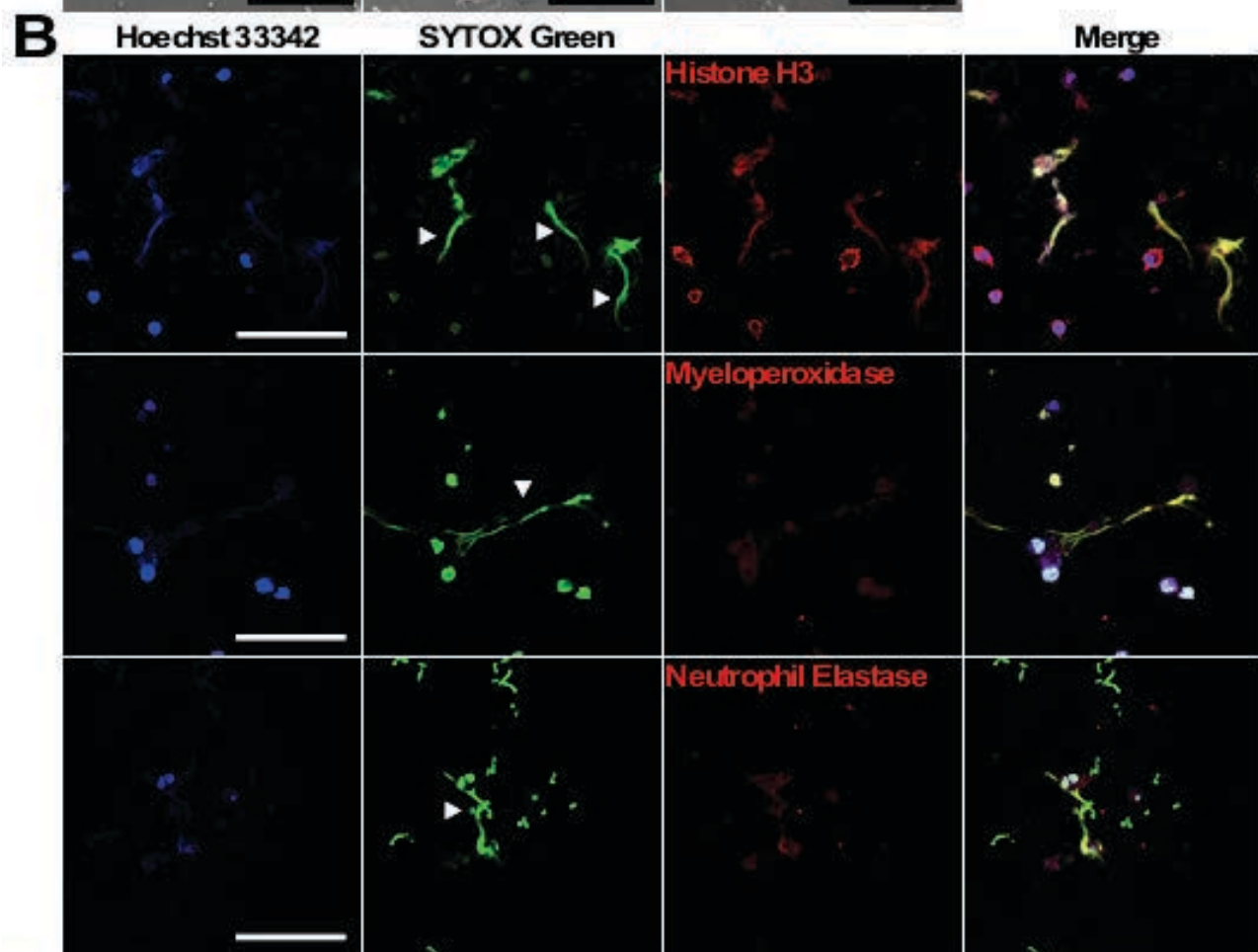
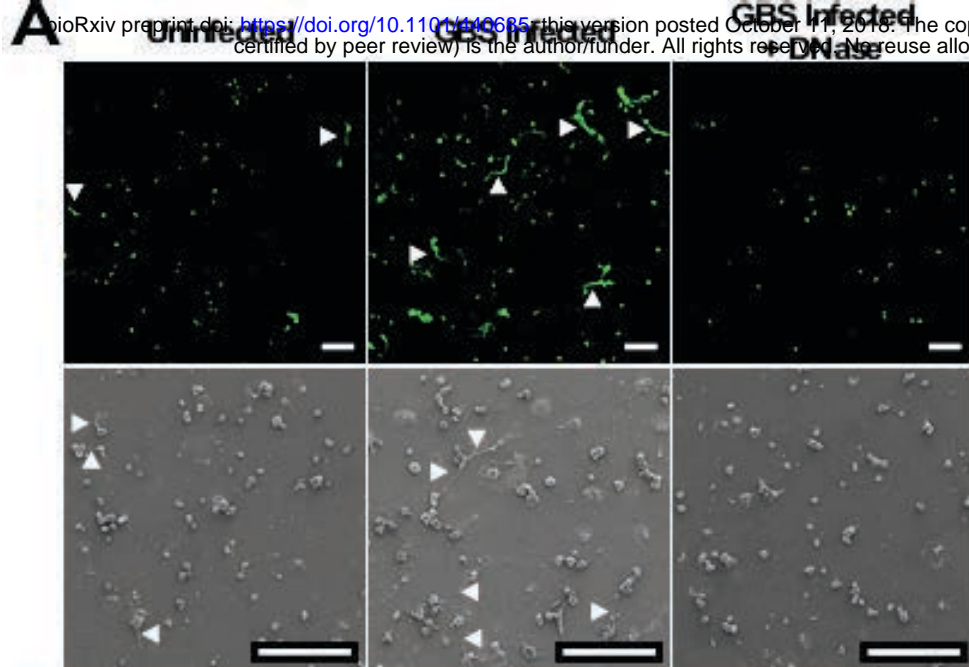
- 330 57. O'Sullivan KM, Lo CY, Summers SA, Elgass KD, McMillan PJ, Longano A, Ford SL, Gan PY,
331 Kerr PG, Kitching AR, Holdsworth SR. 2015. Renal participation of myeloperoxidase in
332 antineutrophil cytoplasmic antibody (ANCA)-associated glomerulonephritis. *Kidney Int*
333 88:1030-46.
- 334 58. Sharma R, O'Sullivan KM, Holdsworth SR, Bardin PG, King PT. 2017. Visualizing Macrophage
335 Extracellular Traps Using Confocal Microscopy. *J Vis Exp* doi:10.3791/56459.
- 336 59. Halder LD, Abdelfatah MA, Jo EA, Jacobsen ID, Westermann M, Beyersdorf N, Lorkowski S,
337 Zipfel PF, Skerka C. 2016. Factor H Binds to Extracellular DNA Traps Released from Human
338 Blood Monocytes in Response to *Candida albicans*. *Front Immunol* 7:671.
- 339 60. Je S, Quan H, Yoon Y, Na Y, Kim BJ, Seok SH. 2016. *Mycobacterium massiliense* Induces
340 Macrophage Extracellular Traps with Facilitating Bacterial Growth. *PLoS One* 11:e0155685.
- 341 61. Aulik NA, Hellenbrand KM, Czuprynski CJ. 2012. *Mannheimia haemolytica* and its leukotoxin
342 cause macrophage extracellular trap formation by bovine macrophages. *Infect Immun*
343 80:1923-33.
- 344 62. Hellenbrand KM, Forsythe KM, Rivera-Rivas JJ, Czuprynski CJ, Aulik NA. 2013. *Histophilus*
345 *somni* causes extracellular trap formation by bovine neutrophils and macrophages. *Microb*
346 *Pathog* 54:67-75.
- 347 63. Perez D, Munoz MC, Molina JM, Munoz-Caro T, Silva LM, Taubert A, Hermosilla C, Ruiz A.
348 2016. *Eimeria ninakohlyakimovae* induces NADPH oxidase-dependent monocyte extracellular
349 trap formation and upregulates IL-12 and TNF-alpha, IL-6 and CCL2 gene transcription. *Vet*
350 *Parasitol* 227:143-50.
- 351 64. Munoz-Caro T, Silva LM, Ritter C, Taubert A, Hermosilla C. 2014. *Besnoitia besnoiti*
352 tachyzoites induce monocyte extracellular trap formation. *Parasitol Res* 113:4189-97.
- 353 65. King PT, Sharma R, O'Sullivan K, Selemidis S, Lim S, Radhakrishna N, Lo C, Prasad J,
354 Callaghan J, McLaughlin P, Farmer M, Steinfert D, Jennings B, Ngui J, Broughton BR, Thomas
355 B, Essilfie AT, Hickey M, Holmes PW, Hansbro P, Bardin PG, Holdsworth SR. 2015.

- 356 Nontypeable *Haemophilus influenzae* induces sustained lung oxidative stress and protease
357 expression. *PLoS One* 10:e0120371.
- 358 66. Chow OA, von Kockritz-Blickwede M, Bright AT, Hensler ME, Zinkernagel AS, Cogen AL,
359 Gallo RL, Monestier M, Wang Y, Glass CK, Nizet V. 2010. Statins enhance formation of
360 phagocyte extracellular traps. *Cell Host Microbe* 8:445-54.
- 361 67. Whidbey C, Vornhagen J, Gendrin C, Boldenow E, Samson JM, Doering K, Ngo L, Ezekwe
362 EA, Jr., Gundlach JH, Elovitz MA, Liggitt D, Duncan JA, Adams Waldorf KM, Rajagopal L.
363 2015. A streptococcal lipid toxin induces membrane permeabilization and pyroptosis leading to
364 fetal injury. *EMBO Mol Med* doi:10.15252/emmm.201404883.
- 365 68. Fettucciari K, Rosati E, Scaringi L, Cornacchione P, Migliorati G, Sabatini R, Fettriconi I, Rossi
366 R, Marconi P. 2000. Group B *Streptococcus* induces apoptosis in macrophages. *J Immunol*
367 165:3923-33.
- 368 69. Liu P, Wu X, Liao C, Liu X, Du J, Shi H, Wang X, Bai X, Peng P, Yu L, Wang F, Zhao Y, Liu M.
369 2014. *Escherichia coli* and *Candida albicans* induced macrophage extracellular trap-like
370 structures with limited microbicidal activity. *PLoS One* 9:e90042.
- 371 70. Jerjomiceva N, Seri H, Vollger L, Wang Y, Zeitouni N, Naim HY, von Kockritz-Blickwede M.
372 2014. Enrofloxacin enhances the formation of neutrophil extracellular traps in bovine
373 granulocytes. *J Innate Immun* 6:706-12.
- 374 71. Neeli I, Dwivedi N, Khan S, Radic M. 2009. Regulation of extracellular chromatin release from
375 neutrophils. *J Innate Immun* 1:194-201.
- 376 72. Touyz RM, Yao G, Quinn MT, Pagano PJ, Schiffrin EL. 2005. p47phox associates with the
377 cytoskeleton through cortactin in human vascular smooth muscle cells: role in NAD(P)H
378 oxidase regulation by angiotensin II. *Arterioscler Thromb Vasc Biol* 25:512-8.
- 379 73. Shao D, Segal AW, Dekker LV. 2010. Subcellular localisation of the p40phox component of
380 NADPH oxidase involves direct interactions between the Phox homology domain and F-actin.
381 *Int J Biochem Cell Biol* 42:1736-43.

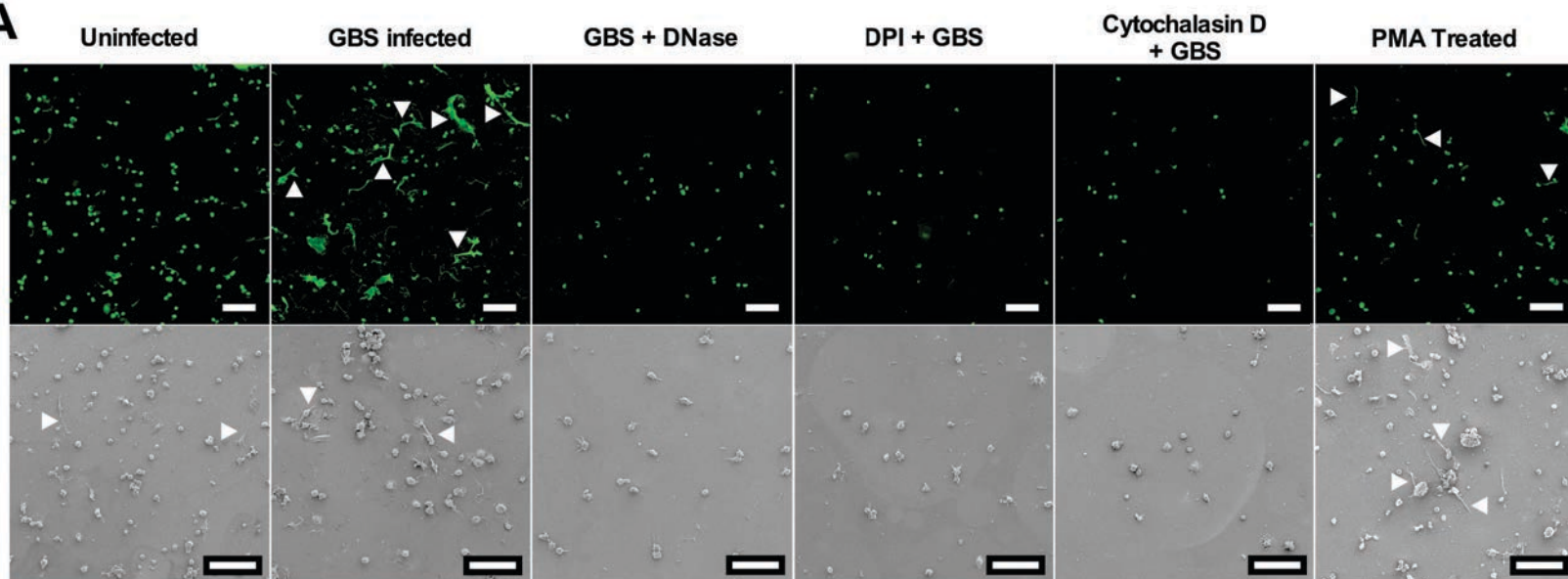
- 382 74. Voloshina EV, Prasol EA, Grachev SV, Prokhorenko IR. 2009. Effect of cytochalasin D on the
383 respiratory burst of primed neutrophils activated with a secondary stimulus. *Dokl Biochem*
384 *Biophys* 424:13-5.
- 385 75. Weiss A, Goldman S, Shalev E. 2007. The matrix metalloproteinases (MMPS) in the decidua
386 and fetal membranes. *Front Biosci* 12:649-59.
- 387 76. Nishihara S, Someya A, Yonemoto H, Ota A, Itoh S, Nagaoka I, Takeda S. 2008. Evaluation of
388 the expression and enzyme activity of matrix metalloproteinase-7 in fetal membranes during
389 premature rupture of membranes at term in humans. *Reprod Sci* 15:156-65.
- 390 77. Kumar D, Moore RM, Mercer BM, Mansour JM, Redline RW, Moore JJ. 2016. The physiology
391 of fetal membrane weakening and rupture: Insights gained from the determination of physical
392 properties revisited. *Placenta* 42:59-73.
- 393 78. Flores-Pliego A, Espejel-Nunez A, Castillo-Castrejon M, Meraz-Cruz N, Beltran-Montoya J,
394 Zaga-Clavellina V, Nava-Salazar S, Sanchez-Martinez M, Vadillo-Ortega F, Estrada-Gutierrez
395 G. 2015. Matrix Metalloproteinase-3 (MMP-3) Is an Endogenous Activator of the MMP-9
396 Secreted by Placental Leukocytes: Implication in Human Labor. *PLoS One* 10:e0145366.
- 397 79. Sundrani DP, Chavan-Gautam PM, Pisal HR, Mehendale SS, Joshi SR. 2012. Matrix
398 metalloproteinase-1 and -9 in human placenta during spontaneous vaginal delivery and
399 caesarean sectioning in preterm pregnancy. *PLoS One* 7:e29855.
- 900 80. Walsh SW, Nugent WH, Solotskaya AV, Anderson CD, Grider JR, Strauss JF, 3rd. 2017.
901 Matrix Metalloprotease-1 and Elastase Are Novel Uterotonic Agents Acting Through Protease-
902 Activated Receptor 1. *Reprod Sci* doi:10.1177/1933719117732162:1933719117732162.
- 903 81. Tambor V, Kacerovsky M, Lenco J, Bhat G, Menon R. 2013. Proteomics and bioinformatics
904 analysis reveal underlying pathways of infection associated histologic chorioamnionitis in
905 pPROM. *Placenta* 34:155-61.

- 906 82. Harris LK, Smith SD, Keogh RJ, Jones RL, Baker PN, Knofler M, Cartwright JE, Whitley GS,
907 Aplin JD. 2010. Trophoblast- and vascular smooth muscle cell-derived MMP-12 mediates
908 elastolysis during uterine spiral artery remodeling. *Am J Pathol* 177:2103-15.
- 909 83. Marder W, Knight JS, Kaplan MJ, Somers EC, Zhang X, O'Dell AA, Padmanabhan V,
910 Lieberman RW. 2016. Placental histology and neutrophil extracellular traps in lupus and pre-
911 eclampsia pregnancies. *Lupus Sci Med* 3:e000134.
- 912 84. Gupta AK, Hasler P, Holzgreve W, Gebhardt S, Hahn S. 2005. Induction of neutrophil
913 extracellular DNA lattices by placental microparticles and IL-8 and their presence in
914 preeclampsia. *Hum Immunol* 66:1146-54.
- 915 85. Gomez-Lopez N, Romero R, Leng Y, Garcia-Flores V, Xu Y, Miller D, Hassan SS. 2017.
916 Neutrophil extracellular traps in acute chorioamnionitis: A mechanism of host defense. *Am J*
917 *Reprod Immunol* 77.
- 918 86. Kothary V, Doster RS, Rogers LM, Kirk LA, Boyd KL, Romano-Keeler J, Haley KP, Manning
919 SD, Aronoff DM, Gaddy JA. 2017. Group B Streptococcus Induces Neutrophil Recruitment to
920 Gestational Tissues and Elaboration of Extracellular Traps and Nutritional Immunity. *Front Cell*
921 *Infect Microbiol* 7:19.
- 922 87. Boldenow E, Gendrin C, Ngo L, Bierle C, Vornhagen J, Coleman M, Merillat S, Armistead B,
923 Whidbey C, Alishetti V, Santana-Ufret V, Ogle J, Gough M, Srinouanprachanh S, MacDonald
924 JW, Bammler TK, Bansal A, Liggitt HD, Rajagopal L, Waldorf KM. 2016. Group B
925 Streptococcus circumvents neutrophils and neutrophil extracellular traps during amniotic cavity
926 invasion and preterm labor. *Sci Immunol* 1.
- 927 88. Carey AJ, Tan CK, Mirza S, Irving-Rodgers H, Webb RI, Lam A, Ulett GC. 2014. Infection and
928 cellular defense dynamics in a novel 17beta-estradiol murine model of chronic human group B
929 streptococcus genital tract colonization reveal a role for hemolysin in persistence and
930 neutrophil accumulation. *J Immunol* 192:1718-31.

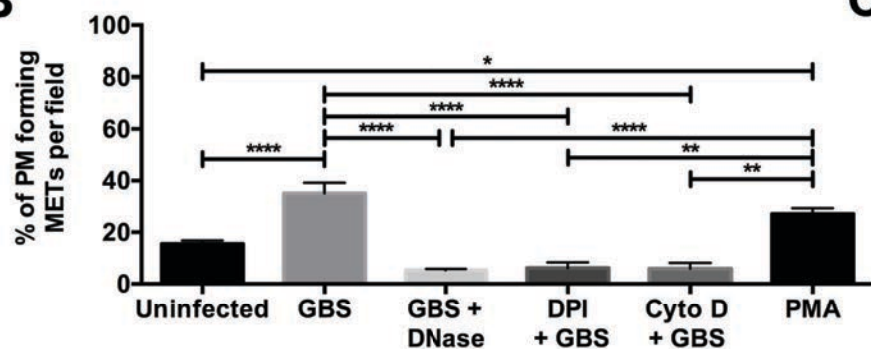
- 931 89. Korir ML, Laut C, Rogers LM, Plemmons JA, Aronoff DM, Manning SD. 2016. Differing
932 mechanisms of surviving phagosomal stress among group B Streptococcus strains of varying
933 genotypes. *Virulence* doi:10.1080/21505594.2016.1252016:1-14.
- 934 90. Manning SD, Lewis MA, Springman AC, Lehotzky E, Whittam TS, Davies HD. 2008. Genotypic
935 diversity and serotype distribution of group B streptococcus isolated from women before and
936 after delivery. *Clin Infect Dis* 46:1829-37.
- 937 91. Gendrin C, Vornhagen J, Armistead B, Singh P, Whidbey C, Merillat S, Knupp D, Parker R,
938 Rogers LM, Quach P, Iyer LM, Aravind L, Manning SD, Aronoff DM, Rajagopal L. 2017. A non-
939 hemolytic Group B Streptococcus strain exhibits hypervirulence. *J Infect Dis*
940 doi:10.1093/infdis/jix646.
- 941 92. Manning SD, Springman AC, Lehotzky E, Lewis MA, Whittam TS, Davies HD. 2009. Multilocus
942 sequence types associated with neonatal group B streptococcal sepsis and meningitis in
943 Canada. *J Clin Microbiol* 47:1143-8.
- 944 93. Iqbal J, Dufendach KR, Wellons JC, Kuba MG, Nickols HH, Gomez-Duarte OG, Wynn JL.
945 2016. Lethal neonatal meningoencephalitis caused by multi-drug resistant, highly virulent
946 *Escherichia coli*. *Infect Dis (Lond)* 48:461-6.
- 947 94. Schindelin J, Arganda-Carreras I, Frise E, Kaynig V, Longair M, Pietzsch T, Preibisch S,
948 Rueden C, Saalfeld S, Schmid B, Tinevez JY, White DJ, Hartenstein V, Eliceiri K, Tomancak
949 P, Cardona A. 2012. Fiji: an open-source platform for biological-image analysis. *Nat Methods*
950 9:676-82.
- 951 95. McCloy RA, Rogers S, Caldon CE, Lorca T, Castro A, Burgess A. 2014. Partial inhibition of
952 Cdk1 in G 2 phase overrides the SAC and decouples mitotic events. *Cell Cycle* 13:1400-12.
- 953 96. Doster RS, Kirk LA, Tetz LM, Rogers LM, Aronoff DM, Gaddy JA. 2017. *Staphylococcus*
954 *aureus* Infection of Human Gestational Membranes Induces Bacterial Biofilm Formation and
955 Host Production of Cytokines. *J Infect Dis* 215:653-657.
- 956



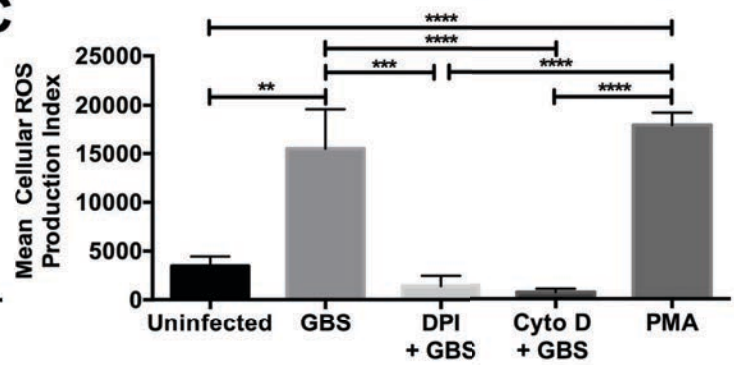
A



B



C



D

